COMPUTER METHODS AND PROGRAMS IN BIOMEDICINE 114 (2014) e46–e59

journal homepage: www.intl.elsevierhealth.com/journals/cmpb

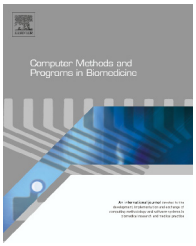

A passive movement method for parameter estimation of a musculo-skeletal arm model incorporating a modified hill muscle model

Tung Fai Yu[a,*], *Adrian J. Wilson*[a,b]

[a] *Department of Physics, University of Warwick, Coventry CV4 7AL, United Kingdom*
[b] *Department of Clinical Physics and Bioengineering, University Hospital Coventry and Warwickshire NHS Trust, Coventry CV2 2DX, United Kingdom*

ARTICLE INFO

Article history:
Received 13 December 2012
Received in revised form
23 October 2013
Accepted 6 November 2013

Keywords:
Passive movement
Musculo-skeletal
Hill muscle model
Joint trajectories
Bicep
Triceps
Parameter estimation

ABSTRACT

In this paper we present an experimental method of parameterising the passive mechanical characteristics of the bicep and tricep muscles in vivo, by fitting the dynamics of a two muscle arm model incorporating anatomically meaningful and structurally identifiable modified Hill muscle models to measured elbow movements. Measurements of the passive flexion and extension of the elbow joint were obtained using 3D motion capture, from which the elbow angle trajectories were determined and used to obtain the spring constants and damping coefficients in the model through parameter estimation. Four healthy subjects were used in the experiments. Anatomical lengths and moment of inertia values of the subjects were determined by direct measurement and calculation. There was good reproducibility in the measured arm movement between trials, and similar joint angle trajectory characteristics were seen between subjects. Each subject had their own set of fitted parameter values determined and the results showed good agreement between measured and simulated data. The average fitted muscle parallel spring constant across all subjects was 143 N/m and the average fitted muscle parallel damping constant was 1.73 Ns/m. The passive movement method was proven to be successful, and can be applied to other joints in the human body, where muscles with similar actions are grouped together.

1. Introduction

In this paper we describe a passive method for parameterising the passive mechanical characteristics of human muscles in vivo. As an example, a study of the movement of the elbow joint and the procedure to obtain parameter values of an arm model incorporating the elbow flexor and extensor muscles as modified Hill muscle models is presented.

The focus for much biomechanical modelling has either been on body segment motion e.g. [1] or on the analysis of individual joint movements e.g. [2]. Whole body models used neural network (NN) or genetic algorithms (GA) to assign muscle forces and properties to individual muscle groups within the body from kinematic measurements e.g. [3,4]. However, limited anatomical and physiological data on individual joints and muscles were incorporated into these models. The majority of the modelling work on single joints has been aimed at

* *Corresponding author at*: Department of Physics, University of Warwick, Coventry CV4 7AL, United Kingdom. Tel.: +44 024 765 23965.
E-mail address: Tung.Yu@warwick.ac.uk (T.F. Yu).
0169-2607
http://dx.doi.org/10.1016/j.cmpb.2013.11.003

understanding the motion around the joint and consequently the majority of the models generated were not predictive.

However predictive models are required for the design of prostheses or orthoses, in particular patient specific prostheses and orthoses. Orthoses and prostheses, including functional electrical stimulation (FES), are only one component of rehabilitation where achieving independence and performing activities of daily living (ADL) is the ultimate goal. Medically and therapeutically, clinicians often wish to use orthoses and prostheses to emphasise or de-emphasise parts of a current movement. Without detailed predictive models that are anatomically and physiologically meaningful, such changes to the movement cannot be incorporated into the prosthesis and orthoses and hence the overall strategy for the patient. Therefore, our goal was to generate musculo-skeletal models where components are physiologically and anatomically meaningful.

One of the stimuli for the current work is the development of models for the design of model based control system for FES systems. FES [5] has been used as part of rehabilitation strategies on spinal cord injured (SCI) patients for regaining movement functions, such as generating knee lock to allow standing, e.g. [6–9], or achieving balance by controlling ankle angle, e.g. [10,11]. Traditionally, many FES systems have used open loop on/off control, e.g. [8]. Such systems are simple to implement and do not require predictive models, however they were found to cause rapid muscle fatigue. For example, Chesler and Durfee's [12] study of maximum tension and fatigue under FES, showed that maximum tension reduced to 50% in about 15 s. Much of the work on closed loop FES controllers has been based on proportional integral derivative (PID), NN or GA controllers. In PID controllers [10], mechanistic models were used, but the bulk parameters had no anatomical and physiological meaning, and control systems were optimised to individual patients empirically. For NN, e.g. [3] and GA, e.g. [4], based controllers, machine learning techniques were required to obtain numerical values, but once again these had no anatomical or physiological meaning.

Irrespective of their purpose, biomechanical models usually contain unknown parameters, where values are determined through parameter estimation techniques. Traditionally, measurements from maximum voluntary contraction (MVC) have been used as part of the parameterisation of muscle models, e.g. [13–15], however, a problem arises if voluntary contraction is not possible, for example when working with SCI subjects. In these cases the MVC method cannot be used. As a solution, we propose an experimental method using passive movements, in which the muscles are completely relaxed and non-active, to obtain numerical values for the passive mechanical parameters in the muscle model. In the case of the bicep and tricep muscles, measurement of passive elbow flexion and extension was used for parameter estimation.

2. Background

Hill type muscle models [16], which are widely used in musculo-skeletal modelling, represent the muscle as a combination of mechanical components. Because these mechanical components model properties that result from a large number of microscopic events, which occur at the sarcomere level, it is not possible to measure the dynamic properties of these components directly for individual subjects in vivo. Therefore, the only approach to obtain parameter values is to use parameter estimation techniques, in which simulated data are fitted to measured data. Currently, few parameter values for the passive mechanical components have been published from studies where parameter values were obtained from measured data in vivo [2,17,18]. In one study [19], a promising approach to parameterising the classical Hill model was presented but these authors were unable to obtain parameter values, although the reasons for this are unclear. We have previously shown that the classical Hill muscle model is not structurally identifiable and therefore parameter values cannot be uniquely obtained through measurement [20]. As part of the same study, we showed that a commonly used modified version of the Hill muscle model [20–24] where there are no serial combinations within the parallel components was structurally identifiable if the internal component lengths of the muscle are known. These latter studies highlighted a further problem in that even where modified Hill muscle models had the same structure, there were inconsistencies between studies in the anatomical definitions of the model components. The anatomical definitions of the modified Hill muscle model used in this study follow those we outlined in the structural identifiability analysis [20] and are described in detail in Sections 3.2 and 4.1.

Our goal was to parameterise individual muscles or group of muscles that are similar in both action and geometry for a particular limb movement, in subjects who had no voluntary control of the muscles for that movement. Since the model follows the anatomy, with the bicep muscle group and tricep muscle working in opposing directions, separate experiments involving movement in each direction are necessary to parameterise the two muscles models. Venture et al. [21,25] have previously reported a similar passive technique for parameterising the elbow joint, however in their study only one experimental protocol was used and their final arm model became a simple 2nd order spring damper model that lacked an explicit muscle model.

The experiments in this study measured the action of passive elbow extension and flexion. Our preliminary results [26] showed the initial elbow extension experiment (denoted experiment 1 in this paper and described in Section 4.2) did not adequately describe the trajectory predicted by the model when maximum elbow extension was reached after 90° of movement. This only gave 0.6 s of data for parameter estimation, therefore in this paper, work on a modified version of the extension experiment (experiment 3) is described, in which a different upper arm orientation is used (see Section 4.4), providing a larger range of elbow angle movements (135°) for parameter estimation.

3. Materials

3.1. *Musculo-skeletal model of the human arm*

The two segment model shown in Fig. 1 is a representation of the human arm [20,26]. It has one degree of freedom around

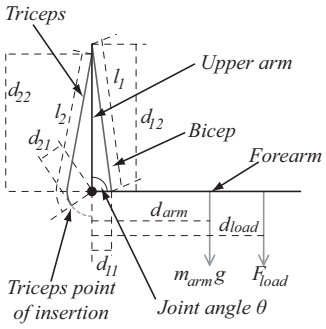

Fig. 1 – Two muscle arm model, showing the flexor bicep muscle and extensor tricep muscle. This arm orientation is the starting arm orientation in experiment 1. The grey dotted arc around the centre of rotation shows the path of the tricep point of insertion and the path of the portion of the tricep free tendon that wraps around the joint when the arm is flexed. The tricep point of insertion rotates around the joint with the forearm.

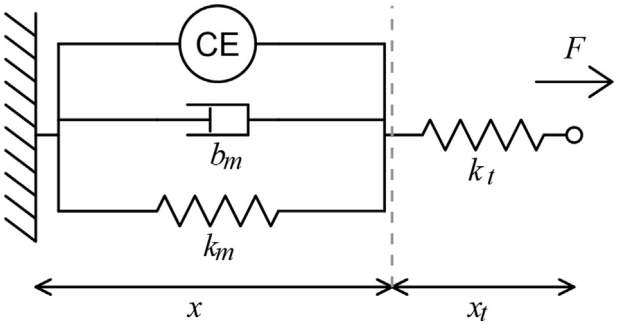

Fig. 2 – Modified parallel Hill muscle model incorporating a free tendon of spring constant k_t, and length x_t. x represents the length of the bulk of the muscle, which has a contractile element CE, damper b_m and spring k_m in parallel.

the elbow joint. The muscles are the flexor muscle, defined as the bicep muscle in this model, which anatomically describes the bicep brachii and brachialis acting in parallel; and the extensor muscle, triceps brachii, defined as the tricep muscles in this model.

The length d_{11}, d_{12}, d_{21} and d_{22} are the distances from the centre of the joint to the points of origin and insertion of the free tendons. The free tendon is that portion of the tendon which is external to the bulk of the muscle (see Section 3.2). It should be noted that anatomically, the point of insertion of the lower end of the triceps tendon attaches to the olecranon which protrudes backwards from the centre of rotation of the joint. During joint extension and flexion, the point of insertion of the tricep rotates around the centre of joint with the forearm, and its movement path is assumed to follow an arc of a circle around the centre of rotation of the elbow joint, with fixed radius of d_{21}. Mechanically, the assumption is that when the elbow flexes, the lower end of the tricep free tendon 'wraps around' structures in the elbow, and the portion of the tendon what wraps around the joint was also assumed to follow a path of an arc around the centre of rotation of the elbow, with a constant radius of d_{21}. In Fig. 1, a dotted line shows the arc of which is the path of the point of insertion around the centre of rotation, and also the path of the portion of the free tendon that wraps around the elbow joint. d_{arm} is the distance between the centre of the elbow joint and the centre of mass of the arm plus hand. d_{load} is the distance from the elbow to the centre of the load force applied to the hand, the latter being the centre of 1 kg or 2 kg weights held in the hand during the experiments. The lengths of the bicep and tricep muscles plus the lengths of the free tendons are defined by l_1 and l_2, and these are described in Section 3.2.

The dynamics of this model are determined by the dynamics of the muscles and the mechanical geometry of the skeletal and soft tissue components, which are described in Sections 3.2 and 3.3.

3.2. *Modified parallel hill muscle model with exposed free tendon*

The mechanical characteristic of the bicep and tricep muscles are represented by a modified parallel element Hill muscle model in series with an exposed free tendon k_t (Fig. 2). The contractile element (CE) represents the force source when the muscle is activated. The damping element b_m represents energy loss within the muscle from mechanical inefficiency at the actin/myosin level. The parallel spring element k_m represents elasticity of the bulk muscle reflecting its ability to return to its natural length. The length x represents the length of the bulk muscle, and x_t represents the length of exposed free tendon. The lengths of the free tendons at both ends of a muscle are summed together and modelled as one serial spring.

Equivalent free tendon spring constants have been reported to lie in the range 60–170 kN/m [27]. The maximum strain of a tendon before failure is about 10%, and it has been suggested that the nominal strain is about 3.3% [28]. The change in the total length of the muscle and free tendon during muscle elongation is much larger than the maximum strain achieved through the free tendon, and therefore the majority of this increase in length comes from the muscle. During passive elongation, a muscle can be stretched to 1.5 times its resting length with minimal force. Therefore the extensions of the free tendons caused by the passive muscle forces are considered negligible in comparison to the extension of the bulk of the muscle and thus the free tendons are assumed to have fixed lengths. The result of this assumption is that when the contractile element CE is not active, the dynamics of the muscle are completely determined by the spring and damping elements. This scenario is used experimentally to allow the parameter values for the passive elements to be determined.

3.3. *System equations*

Euler's second law has been used to derive the system equations for the musculo-skeletal models shown in Fig. 1. The system Eqs. (1)–(9) describe the elbow joint dynamics when the arm is in the same orientation as shown in Fig. 1. The contractile element in the muscle model (Fig. 2) is assumed to be a

pure force generator and therefore plays no part in the dynamics of the model. The upper arm is fixed in a vertical position and with the muscle not activated, the forearm and hand are allowed to swing, pivoted around the elbow. The wrist is fully extended at all times. Starting with the angular velocity and acceleration, the equations of motions are:

$$\dot{\theta} \equiv \frac{d\theta}{dt} \tag{1}$$

$$\ddot{\theta} \equiv \frac{d\dot{\theta}}{dt} = \left(\frac{\tau_{\lim 1} + \tau_{\lim 2} + F_1((d_{11}d_{12}\ \sin\theta)/l_1) - F_2 d_{21} + m_{arm} d_{arm} g\ \sin\theta + m_{load} d_{load} g\ \sin\theta - b_{arm}\dot{\theta}}{J} \right) \tag{2}$$

where the angular acceleration $\ddot{\theta}$ equals to the sum of torques divided by the moment of inertia. d_{11}, d_{12}, d_{21}, d_{22}, d_{arm}, d_{load} and θ are defined in Fig. 1. A damping factor b_{arm} represents the resistance to movement caused by soft tissues around the elbow joint. τ_{lim1} and τ_{lim2} are the torques at the joint limits and are described at the end of this section and modelled by Eqs. (8) and (9). The third and fourth terms in (2) (terms containing F_1 and F_2 respectively) are the torques from the bicep and tricep muscles, which are products of the moment arm and the passive force of the muscles under elongation in the direction perpendicular to the forearm.

The bicep moment arm is d_{11}, and the perpendicular force is the bicep force adjusted by the direction of the muscle and angle of the elbow, derived from the geometry in Fig. 1. As described in Section 3.1, when the elbow is flexed, a portion of the lower free tendon of the tricep muscle wraps around the elbow, following the path of an arc with constant radius of d_{21} from the centre of rotation. Since the free tendon always leaves this arc tangentially, the tricep muscle force, F_2, always acts tangentially to the path of this arc, and the moment arm of this force is the radius of the arc, which is always equal to d_{21}. The two terms following the muscle torques are the torques caused by gravity acting on the mass of the arm and any weights held in the hand. J is the moment of inertia of the forearm together with any extra weight held in the hand, calculated using Eq. (12), see Section 4.1.

From Fig. 2, the bicep muscle force F_1 and tricep muscle force F_2 are given by:

$$F_i = F_{CEi} + b_{mi}\dot{x}_i + k_{mi}(x_i - x_{i\_0}),\ i = 1, 2 \tag{3}$$

where x_{1_0} and x_{2_0} are the natural length of the bicep and tricep muscles, excluding the length of the free tendons. As described in Section 3.2, the free tendons are assumed to have fixed lengths, but when the geometry of the model gives lengths shorter than their fixed lengths, they become slack. This means the free tendons can only transfer contractile force and therefore if $F_i \le 0$, $F_i = 0$ in (3).

It should be noted that (2) is a generalised equation for the movement of the joint with the upper arm in the position shown in Fig. 1. In voluntary elbow flexion, F_1 is active and F_2 only contributes a passive (resistive) force and vice versa for extension. However in this work, only passive movements are being considered and therefore the voluntary forces of the muscles, F_{CE}, in (3) are zero at all times.

From Fig. 2, the bicep muscle length x_1, its velocity of contraction $\dot{x}_1$, the tricep muscle length x_2 and its velocity of contraction $\dot{x}_2$ are given by:

$$x_1 = l_1 - x_{1t} = \sqrt{{d_{11}}^2 + {d_{12}}^2 - 2d_{11}d_{12}\ \cos\theta} - x_{1t} \tag{4}$$

$$\dot{x}_1 \equiv \frac{dx_1}{dt} = (d_{11}^2 - d_{12}^2 - 2d_{11}d_{12}\ \cos\theta)^{-0.5} \cdot d_{11}d_{12}(\sin\theta)\dot{\theta} \tag{5}$$

$$x_2 = l_2 - x_{2t} = \sqrt{d_{22}^2 - d_{21}^2} + d_{21}(\pi - \theta) - x_{2t} \tag{6}$$

$$\dot{x}_2 \equiv \frac{dx_2}{dt} = -d_{21}\dot{\theta} \tag{7}$$

where x_{1t} is the bicep free tendon length and x_{2t} is the tricep free tendon length.

Additional torques resulting from soft tissue compression and extension are present near the maximum angle of flexion and extension respectively: τ_{lim1} represents additional torque at maximum extension; and τ_{lim2} represents additional torque at maximum flexion, and are modelled as:

$$\tau_{\lim 1} = \begin{cases} -k_{\lim}(\theta - \theta_{\lim 1}) - b_{\lim}\dot{\theta} & \text{if } \theta > \theta_{\lim 1} \text{ and } \dot{\theta} > 0 \\ -k_{\lim}(\theta - \theta_{\lim 1}) & \text{if } \theta > \theta_{\lim 1} \text{ and } \dot{\theta} \le 0 \\ 0 & \text{if } \theta \le \theta_{\lim 1} \end{cases} \tag{8}$$

$$\tau_{\lim 2} = \begin{cases} -k_{\lim}(\theta - \theta_{\lim 2}) - b_{\lim}\dot{\theta} & \text{if } \theta < \theta_{\lim 2} \text{ and } \dot{\theta} < 0 \\ -k_{\lim}(\theta - \theta_{\lim 2}) & \text{if } \theta < \theta_{\lim 2} \text{ and } \dot{\theta} \ge 0 \\ 0 & \text{if } \theta \ge \theta_{\lim 2} \end{cases} \tag{9}$$

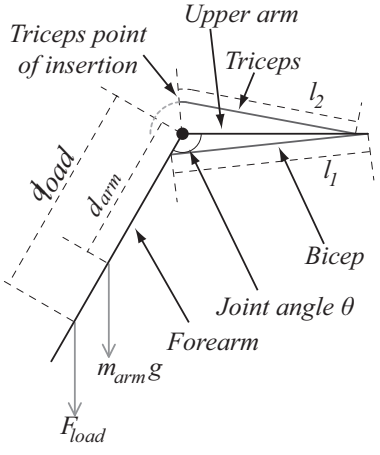

Fig. 3 – Two muscle arm model, showing the arm in the orientation used in experiment 2 to measure elbow flexion. The upper arm is held horizontal and the forearm is allowed to swing. The points of origin and insertions of the muscles are not shown in this figure but are identical to Fig. 1.

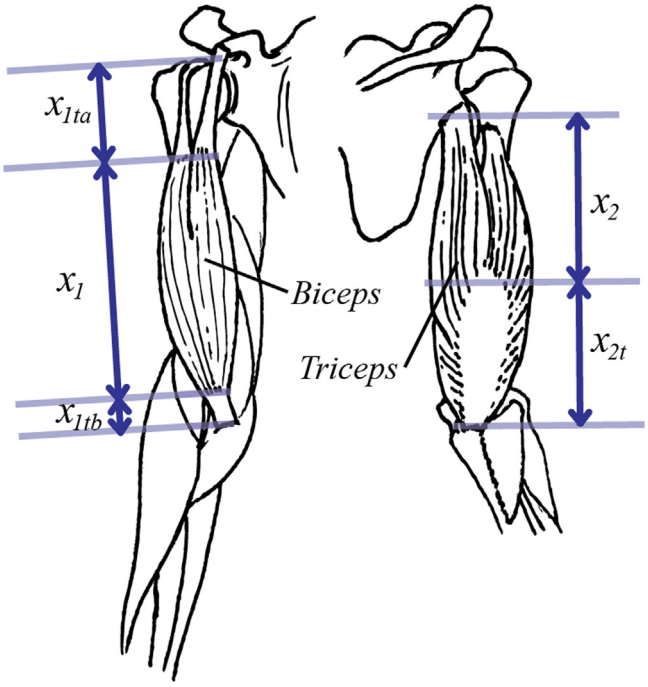

Fig. 4 – Definition of free tendon length and bulk muscle length. Exposed free tendon of the biceps is the sum of x_{1ta} and x_{1tb}. Sum of muscle and free tendon length equals to l_1 and l_2.

where k_{lim} and b_{lim} represent the effective rotational spring and damping constants of the soft tissue, which are assumed to be the same for both extension and compression.

Eq. (2) analyses extension at the elbow joint. To analyse flexion, the upper arm needs to be in a horizontal plane with the elbow facing upwards, see Section 4.3, Fig. 3 and Fig. 5b. $\ddot{\theta}$ is now given by Eq. (10) to reflect the difference in the direction of gravity with reference to the elbow angle.

$$\ddot{\theta} \equiv \frac{d\dot{\theta}}{dt} = \left(\frac{\tau_{\lim 1} + \tau_{\lim 2} + F_1((d_{11}d_{12}\sin\theta)/l_1) - F_2 d_{21} + m_{arm}d_{arm}g\cos\theta + m_{load}d_{load}g\cos\theta - b_{arm}\dot{\theta}}{J} \right) \quad (10)$$

In our preliminary results for experiment 1 (Fig. 1) [26], the arm swing movement is limited by maximum elbow extension, to overcome this, a third experimental setup was used. Described in Section 4.4, experiment 3, the arm starts in a position where the upper arm was leaned forward by 45° from vertical, see Fig. 5c. For this orientation, $\ddot{\theta}$ is given by Eq. (11)

$$\ddot{\theta} \equiv \frac{d\dot{\theta}}{dt} = \left(\frac{\tau_{\lim 1} + \tau_{\lim 2} + F_1((d_{11}d_{12}\sin\theta)/l_1) - F_2 d_{21} + m_{arm}d_{arm}g\sin(\theta + (\pi/4)) + m_{load}d_{load}g\sin(\theta + (\pi/4)) - b_{arm}\dot{\theta}}{J} \right) \quad (11)$$

4. Experiment protocol

Four healthy subjects participated in the experiments, where none of the subjects had any known bone, muscle or nerve disease. Whilst the primary stimulus of this work was FES, Mohammed et al. [19] reported that muscle characteristics do not differ between the healthy subjects and SCI subjects when carrying out SCI studies, and therefore normal healthy subjects with no diagnosed muscle, bone or joint diseases could be used in this study. Height and weight characteristics of the subject are included in Table 2.

The length and mass parameters can be directly measured or calculated. The method of measurement is described in Section 4.1. The arm model (see Fig. 1) and system equations in Section 3.3 describe a model containing an antagonist pair of muscles allowing flexion and extension of the forearm. Therefore different experimental procedures observing extension (experiment 1 and 3) and flexion (experiment 2) are necessary to determine parameters that are not directly measurable, i.e. the spring and damping constants in Eqs. (2), (3), (8)–(11).

These experiments are designed to examine the step response of the elbow joint and determine the system parameters. As described in Section 3.2, measuring motion when the muscles are inactive allows the parameter values of the passive components in the arm and the muscles to be determined. To achieve this, free fall motions were used in all experiments. The basic principle was to initially support the forearm by a trigger block, where the forearm has potential energy, see Fig. 5. By quickly (assumed to be instantaneously) removing the trigger block from under the wrist while the muscles are completely relaxed, the elbow joint experiences a step change in net moment, and extends or flexes due to gravity acting on the mass of the arm, hand and any mass held. The experiments are described in Sections 4.2–4.4.

A Vicon biomechanical 3 dimensional (3D) motion capture system [29] was used to measure the segment trajectories. The Vicon system captures at 200 frames per second and has a resolution of 0.1 mm. An 8 markers configuration was used to locate the 3D position of the shoulder, elbow, wrist and hand. Markers were also placed on the trigger block to allow removal of the block to be captured. The placements of the arm markers are listed in Table 1. Fig. 5 contains images from the experiments showing the locations of the markers. The measured marker positions were used to compute the centre of the joints and elbow angles, these calculations are described in Section 4.5.

4.1. Anatomical parameter measurement and calculation

The directly measurable parameters in the system equations given in Section 3.3 are d_{11}, d_{12}, d_{21}, d_{22}, l_{arm}, r_{arm}, d_{load}, x_{1t}, x_{2t}, x_{1_0} and x_{2_0}. Palpation and surface measurement were used to determine the anatomical lengths; with a resolution of 5 mm. Fig. 4 was used as a guide for measuring free tendon lengths. Average values from five consecutive measurements were used. Distance d_{arm} was derived from l_{arm} using a table of anthropometric data [30]. The distance d_{load} was measured

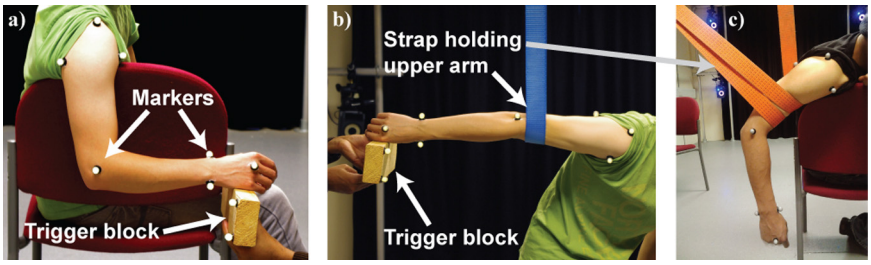

Fig. 5 – (a) Experiment 1, 90° elbow extension starting position with trigger block supporting the hand. Some markers and the trigger block are labelled. (b) Experiment 2 flexion starting position with trigger block supporting the hand and strap holding the upper arm. (c) Experiment 3, 45° flexion experiment, showing the upper arm fixed by a strap. This is the resting position of the arm at the end of the experiment. The ElbIn marker is on the medial side of the elbow and not visible in these images.

Table 1 – Arm markers used in 3D motion capture.

Marker name	Description and marker placement
ShoTop	Top of shoulder, placed on top of the highest point of the acromion
ShoFro	Front of shoulder, place in front of the shoulder align with the anterior–posterior line that pass through the centre of the shoulder joint rotation.
ShoRea	Front of shoulder, place behind the shoulder align with the anterior–posterior line that pass through the centre of the shoulder joint rotation
ElbOut	Outside of elbow, placed on the lateral side of the elbow aligned with the medial lateral elbow centre of rotation line
ElbIn	Inside of elbow, placed on the medial side of the elbow aligned with the medial lateral elbow centre of rotation line
WriA	Wrist marker A, placed on the styloid process of radius
WriB	Wrist marker B, placed on the styloid process of ulna
Hand	Hand marker, placed on the back of the hand on top of the head knuckle of the middle finger metacarpal

from the centre of the elbow joint to the centre of the mass held in the hand.

To calculate the segment mass and moment of inertia, the forearm and the hand are assumed to be cylindrical with the mass uniformly distributed. The mass of the forearm together with the hand, m_{arm}, was measured by supporting the elbow and weighing the arm with the muscles fully relaxed at the 2nd knuckle of the middle finger. From the uniform mass distribution assumption, m_{arm} is twice the mass value obtained from weighing. The moment of inertia of the forearm and hand J in (2), (10) and (11) was then calculated by using the following standard approximation for a cylindrical object

$$J = \frac{1}{4}m_{arm}r_{arm}^2 + \frac{1}{3}m_{arm}l_{arm}^2 + m_{load}d_{load}^2 \quad (12)$$

where the length of the cylinder l_{arm} was measured from the centre of the elbow joint to the 2nd knuckle of the middle finger with the hand clenched as a fist. The radius of the arm r_{arm} is approximated as half the diameter of the forearm,

Table 2 – Measured parameters of four subjects.

Subject parameters	P1	P2	P3	P4
Height (m)	1.65	1.75	1.80	1.70
Weight (kg)	55	74	75	54
Forearm + hand weight (kg)	0.92	1.28	1.88	0.96
d_{11} (mm)	45	50	37.5	45
d_{12} (mm)	269	285	250	275
d_{21} (mm)	45	50	55	50
d_{22} (mm)	240	255	248	248
x_{1t} (mm)	100	116	120	112
x_{2t} (mm)	123	130	135	126
x_{1_0} (mm)	146	150	155	145
x_{2_0} (mm)	155	161	140	156
l_{arm} (mm)	340	370	380	340
d_{arm} (mm)	150	163	168	152
d_{load} (mm)	330	360	330	292
r_{arm} (mm)	35	39	40	35
J (kg m^2), 0 kg in hand	0.0279	0.0589	0.0912	0.0373
J (kg m^2), 1 kg in hand	0.133	0.168	0.200	0.137
J (kg m^2), 2 kg in hand	0.246	0.277	0.309	0.235

measured at 1/3rd of the distance from the elbow to the wrist. The moment of inertia is assumed to be constant over time.

4.2. *Forearm free fall experiment 1 – elbow extension*

This experiment examines the forearm free fall trajectory during arm extension. It begins with the subject's right arm positioned in the orientation shown in Figs. 1 and 5a. The upper arm is held vertical at all times and the forearm starts from an elbow angle of 90°, which is supported by the trigger block placed under the hand.

The hand is placed on the trigger block in the orientation as shown in Fig. 5. This is the neutral pronation/supination (PS) angle of the forearm and hand when the bicep brachii is relaxed.

When the trigger block is removed, the forearm and hand fall freely under gravity. The arm is expected to reach maximum extension and then rebound before eventually coming to rest. The length of recorded data for each trial was 10 s, where the trigger block was removed after a random time delay of up to 5 s after the start of data recording.

Three separate hand loads were used: zero load, 1 kg or 2 kg weights held in the hand. For each subject and experiment, consecutive trials were carried out in the following order: 5 trials with 0 kg added to the hand, 5 trials with 1 kg held in the hand, 3 trials with 2 kg held in the hand and 3 trials with 0 kg added to the hand. A smaller number of trials were done with 2 kg to minimise the possibility of fatigue in the hand. The last 3 trials of 0 kg load were carried out to ensure the passive characteristics of the arm and muscle had not changed due to the duration of the experiment and the initial measured trajectories of 0 kg hand load were reproducible.

4.3. *Forearm free fall experiment 2 – elbow flexion*

Experiment 2 records the subject's forearm free fall trajectory for flexion. The subject's arm starting position in experiment 2 is shown in Fig. 5b. The upper arm is held horizontal by a strap with elbow facing up at all times and the forearm starts from maximum extension supported by the trigger block placed under the hand. When the trigger block is removed downwards, the elbow joint flexes freely, with the motion being similar to a damped pendulum motion. The recording procedure including the trial length, random delay before removing trigger block, load applied to the hand and the number of measurements taken was identical to the protocol used in experiment 1.

4.4. *Forearm free fall experiment 3 – 45° elbow extension*

Experiment 3 measures the forearm free fall trajectory (elbow extension) similar to experiment 1, however in experiment 3 the orientation of the upper arm was at 45° from the vertical position, held by a strap, see Fig. 5c. The trigger block initially holds the forearm in a horizontal position, where the elbow angle is at 45°, the trigger block was removed downwards in the same fashion as in experiment 1 and 2 to start the experiment. The recording procedure including the trial length, random delay before removing trigger block, load applied to the hand and the number of measurements taken was identical to the protocol used in experiments 1 and 2.

4.5. *Measured data preparation for parameter estimation*

The measured elbow angle was computed on a frame by frame basis using the measured arm marker positions. First the centre of the shoulder joint (SHO), elbow joint (ELB) and wrist joint (WRI) were calculated from the 3D location of the measured marker positions (13)–(15), where the marker names refer to the markers detailed in Table 1.

$$\mathrm{SHO} = \left(\frac{ShoTop + ShoFro + ShoRea}{3}\right) \tag{13}$$

$$\mathrm{ELB} = \left(\frac{ElbOut + ElbIn}{2}\right) \tag{14}$$

$$\mathrm{WRI} = \left(\frac{WriA + WriB}{2}\right) \tag{15}$$

The elbow angle was then calculated as the acute angle between the upper arm vector A and forearm vector B (18), where the upper arm vector was from ELB to SHO (16) and the forearm vector was from ELB to WRI (17).

$$A = SHO - ELB \tag{16}$$

$$A = WRI - ELB \tag{17}$$

$$\theta_{elbow} = \cos^{-1}\left(\frac{A \cdot B}{|A||B|}\right) \tag{18}$$

Measurements with missing marker data or where the muscles were not fully relaxed were excluded from parameter estimation. The start of each experiment was identified by locating the instant when the trigger block markers moved downward.

5. Parameter estimation by forward dynamics simulation

Parameter estimation and optimisation was done on a subject by subject basis, to find a set of fitted parameter values of b_{arm}, k_{m1}, k_{m2}, b_{m1}, b_{m2}, k_θ, and b_θ that gave minimum absolute error (MAE) between measured and simulated elbow angle trajectories, the latter of which were generated by simulating a forward dynamic model created from the equations in Section 3.3.

Simulated elbow joint angle and angular velocity time histories for (2), (10) and (11) were obtained by numerically integrating the forward dynamic model using a variable time step Runge–Kutta method ordinary differential equation (ODE) solver (ODE45, Matlab®). All computational work was carried out in Matlab® R2009b.

The error between the measured and simulated elbow angle trajectories was assessed using the MAE. Only experiments 2 and 3 were used to calculate MAE. In each recorded trial the 2 s of data following trigger block removal was used to calculate the MAE, see Eq. (19). For each subject, repeated

Table 3 – Fitted muscle parameter values.

	P1	P2	P3	P4
b_{arm} (Nms/rad)	0.221	0.285	0.114	0.126
k_{m1} (N/m)	207	218	21.4[a]	41.4[a]
b_{m1} (Ns/m)	0.0395	0.188	0.920	0.110
k_{m2} (N/m)	126	148	389[a]	0.419[a]
b_{m2} (Ns/m)	1.99	0.192	5.88	4.57
k_{lim} (Nm/rad)	0.0361	0.0436	2.33	1.13×10^{-6}
b_{lim} (Nms/rad)	6.00×10^{-3}	0.306	0.0733	0.0106
MAE (rad)	0.185	0.174	0.186	0.254

[a] See discussion in Section 7.5.

trials from each experimental configuration (e.g. exp2 0 kg) were averaged to give an average time history to be compared with the corresponding simulated arm fall movement and hand load configuration (e.g. simulated exp2 0 kg), this gave 6 averaged measured trajectories and 6 simulated trajectories. The 6 pairs of data were used to calculate 6 MAEs, and these were then averaged to give an overall MAE for the subject (20). The reason for excluding experiment 1 from the MAE calculation is discussed in Section 7.

$$MAE_{Expi,j\,kg} = \frac{\sum_{t=0\,s}^{2\,s} \left|\theta_{t,average\ \ measured,Expi,j\,kg} - \theta_{t,simulated,Expi,j\,kg}\right|}{t}$$

$$i = 2, 3, \quad j = 0, 1, 2 \tag{19}$$

$$\text{Overall}\quad MAE = \frac{\sum_{i=2}^{3}\sum_{j=2}^{2} MAE_{Expi,jkg}}{6} \tag{20}$$

Parameter estimation was carried out using a multi-dimensional unconstrained nonlinear optimisation method (fminsearch, Matlab®), which minimised the overall MAE of each subject starting from an initial set of parameters (the seed).

Free tendon spring constants had been reported to lie in the range 60–170 kN/m [27], and the stiffness of the free tendon is considered to be much greater than the stiffness of muscle springs, and therefore we assumed the physiologically realistic values for the spring constants (k_{m1}, k_{m2} and k_{lim}) were in the range 0–1000 N/m and 0–1000 Nm/rad. The extreme values for the damping factors (b_{arm}, b_{m1}, b_{m2}, and b_{lim}) were assumed to be 0 and 100 Ns/m (corresponding to 0 and 100 Nms/rad) and values outside this range were rejected.

The parameter estimation for each subject was a two stage process. For the first stage, optimisation was performed for 3 different seeds, to ensure a global minimum MAE was found, these seeds are: fitted values from preliminary work; physiologically realistic values; and all zeros values. For each of these seeds the optimiser was run and the parameter values corresponding to the minimum value of MAE obtained from the 3 seeds was then used as the first seed for the start of the second, iterative stage of the parameter estimation process. In the second stage of the parameter estimation process values of the MAE obtained at the end of each cycle of optimisation were reduced to 3 significant figures (s.f.) and, if different from those obtained from the previous cycle, input as the seed into the next iterative cycle of optimisation. The fitted parameter values were those for which repeated cycles of optimisation produced no change in the 3 s.f. of the MAE values.

6. Results

The measured parameters together with the values of moment of inertia derived from the measurements are given in Table 2. The optimal parameter values obtained by parameter estimation and optimisation are listed in Table 3. In Eqs. (8) and (9), the boundary angles in this study were established by measuring the range of unrestricted movement on one subject, P1. The values obtained were: $\theta_{lim1} = 2.618$ rad (150°) and $\theta_{lim2} = 0.873$ rad (50°).

The 3 initial sets of seeds used were the reported fitted values in previous work [26]: all zero values; and the physiological realistic seed based on the range listed in Section 5, the latter was arbitrarily selected as b_{arm}, b_{m2} and $b_{lim} = 0.5$ Nms/rad, 0.5 Ns/m and 0.5 Nms/rad respectively, $k_{m1} = k_{m2} = 90$ N/m, $b_{m1} = 0.3$ Nms/rad and $k_{lim} = 0.2$ Nm/rad.

With the exception of 1 subject, the 3 seeds gave MAE values that were within 1% for each subject after the initial stage of the parameter estimation process. For P4, using the seed values from previous work and physiologically realistic values yielded MAE values within 1% after the initial stage of parameter estimation. However, the seed with all zero values gave a MAE which converged to a local minimum. Importantly the initial seeds for all subjects gave MAE values that were taken forward to the second, iterative stage of the parameter estimation process.

Simulated elbow angles using the values from Table 3, and the measured elbow angle data are plotted in Figs. 6–9.

7. Discussion

This study has covered a number of aspects of the problem of obtaining parameter values for individual muscles or groups of muscles with similar actions and geometries that control movement of a single joint. Overall the work reported produced numerical values for the joint parameters, and the discussion will be organised to highlight different parts of the process.

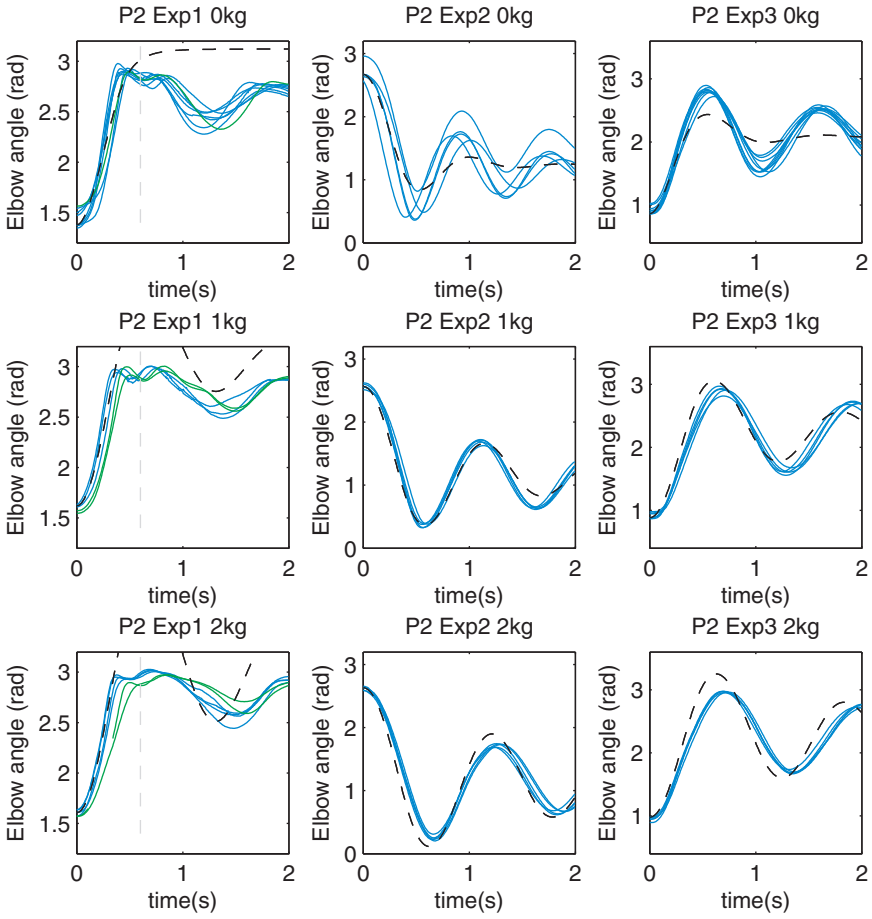

Fig. 6 – Forearm free fall trajectory of subject P1. Blue solids lines: measured joint trajectories. Black dashed line: simulated joint trajectory using values from Tables 2 and 3. (For interpretation of the references to colour in this figure legend, the reader is referred to the web version of the article.)

7.1. *Arm model*

The arm model used in this work simplifies the movement of the elbow and only considers the movement in the flexion and extension direction. The movement in these two directions are governed by all the muscles that are connected around the elbow joint.

The extensor of the elbow consists of the triceps brachii. Although there are more than one point of origin and more than one point of insertion for this muscle, the muscle is commonly modelled or measured using average muscle length, e.g. [31], and that is the approach used in this work.

The arm model of this work (Fig. 1) contains only a single flexor muscle. Anatomically, three muscles cause flexion at the elbow: the bicep brachii, brachialis and brachioradialis. Of these, the bicep brachii and brachialis contribute the majority of the force [31]. These two muscles are of similar length [31,32], overlay each other and act in the same direction. Therefore they have similar moment arms. By fitting the model with only 1 flexor muscle, the mechanical property of both the bicep brachii and brachialis have been combined into the model's bicep muscle. In practice it would be impossible to measure the length of the brachialis in vivo using palpation and surface measurement as it is embedded under the bicep brachii.

Although the arm model used in this work does not reflect the true anatomy of the flexors of the elbow, further structural identifiability analysis of arm models with multiple flexors showed that parameter estimation would not produce unique parameter values for these muscles as they effectively act in parallel. This inability to obtain unique parameter values may explain the reason why Venture et al. [21] failed to obtain parameter values for their model, with the result they subsequently excluded any form of Hill muscle models from their work [25].

7.2. *Experiment design*

Some form of support to the arm is needed to ensure it is in the correct position and orientation. The movement of the upper arm must be minimised, whilst the elbow and forearm are allowed to swing freely without restriction.

Using a strap to position the upper arm was chosen over methods where the elbow joint is held, as any elbow support may restrict motion. In addition, the strap has a minimal physical volume in comparison to frame based supports and

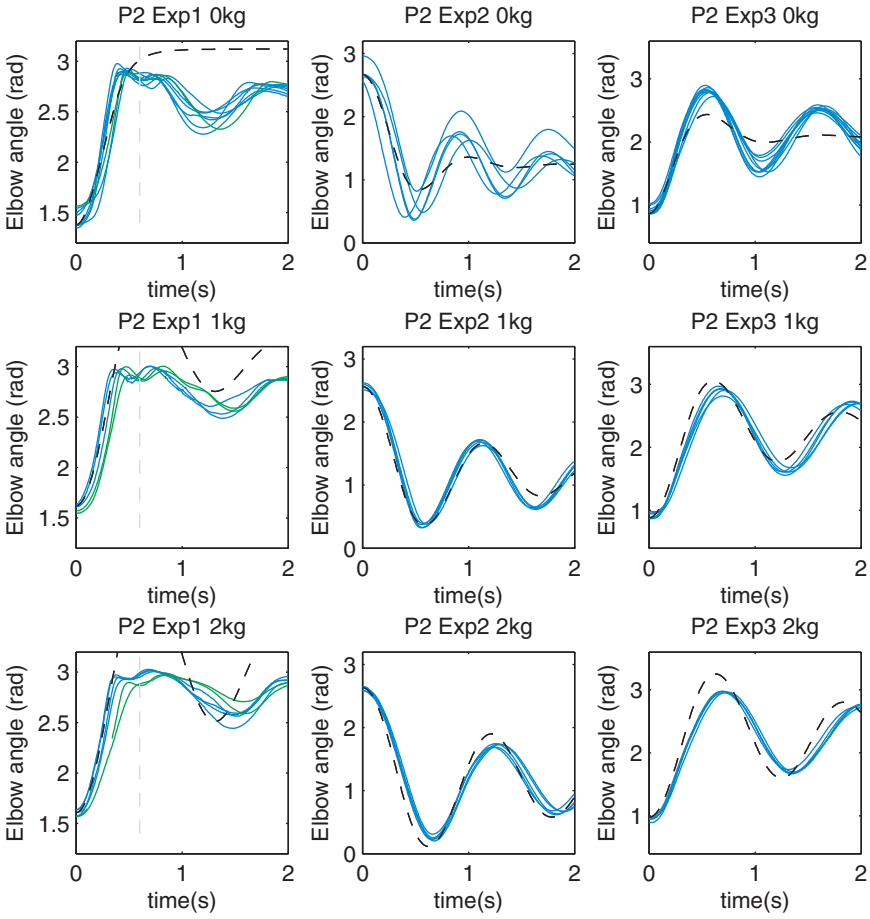

Fig. 7 – Forearm free fall trajectory of subject P2. Blue and green solids lines: measured joint trajectories from different days. Black dashed line: simulated joint trajectory using values from Tables 2 and 3. (For interpretation of the references to colour in this figure legend, the reader is referred to the web version of the article.)

therefore the elbow angle range was not limited by the support. The width of the strap used in the experiments was a compromise between spreading the load and minimising the peak pressure beneath it and thus the pressure on the bicep muscle. The strap was positioned below the bulk of the bicep muscle as shown in Fig. 5 to minimise pressure from the strap on the muscle.

The bicep brachii is also involved in the PS rotation of the forearm, wrist and hand. Placing the hand in a neutral position, as seen in Fig. 5a and b, eliminated any PS rotation of the forearm and hand during the free fall. Therefore the change in length of the bicep brachii is only due to flexion/extension of the elbow and not pronation or supination of the forearm and hand.

The addition of a 1 kg or 2 kg hand load in the experiments greatly reduced the uncertainty in the estimated moment of inertia of the forearm and hand (Table 2). For 1 kg and 2 kg hand load, the estimated moment of inertia values of the forearm and hand, calculated using a cylindrical assumption, were of about 11–45% of the total moment of inertia, and the uncertainty of the moment of inertia of the hand load around the elbow joint was reduced, as the weight and distance between the weight and centre of elbow were directly measured. Therefore it was expected that the simulated trajectory became more accurate as the hand load increased, potentially giving better agreement between the model and measured data. This can be seen in Figs. 6–9 where 1 kg and 2 kg hand load showed better agreement between measured and simulated results than 0 kg hand load. This method provided an alternative to the method of adjusting moment of inertia used by Hof [33], which involved using the recorded moment and angular acceleration to correct the moment of inertia.

We have previously reported preliminary results of the arm fall experiments that only included experiments 1 and 2 [26]. It was found that for experiment 1, the system Eqs. (8) and (9) cannot adequately describe elbow angle trajectory when maximum extension was reached at about 0.4 s (see Figs. 6–9, experiment 1), giving only 0.6 s of data for parameter estimation (see Section 7.4). The problem caused by the joint reaching maximum extension or flexion was also experienced by Hof [2], who limited the period over which they could analyse data to 60 ms. Using a modified form of the passive extension experiment (experiment 3), where the upper arm was leant forward by 45° from the vertical, allowed the forearm to swing further backwards, this gave a larger range of elbow angle for parameter estimation (about 135° whereas 90° was seen in experiment 1). The measured trajectories from experiment 3 (Figs. 6–9) showed the maximum extension was not reached in any of

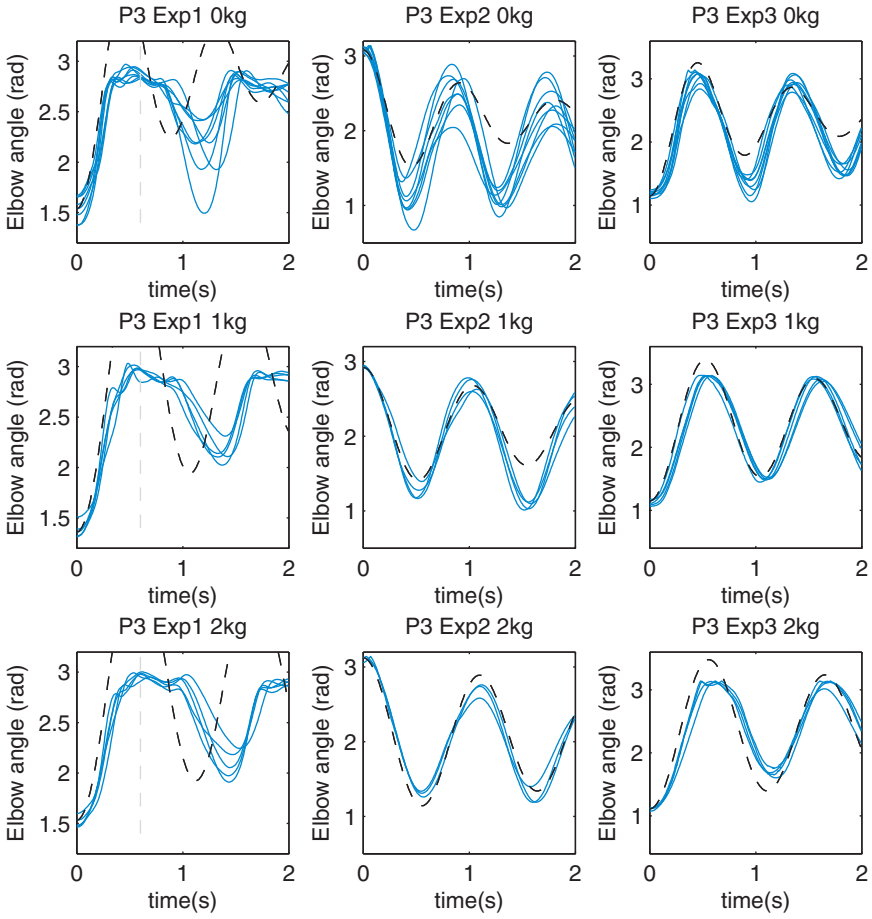

Fig. 8 – Forearm free fall trajectory of subject P3. Blue solids lines: measured joint trajectories. Black dashed line: simulated joint trajectory using values from Tables 2 and 3. (For interpretation of the references to colour in this figure legend, the reader is referred to the web version of the article.)

the trials, and therefore this did not limit the duration of data available for MAE calculation and parameter estimation.

7.3. *Measured results*

Surface palpation was used to determine the free tendon and muscle resting length parameters in this study. In future work, medical imaging technique such as ultrasound or magnetic resonance imaging (MRI) could potentially improve the accuracy of these parameters. A study of this type together with a formal sensitivity analysis of the model would allow the validity of the palpation method to be further assessed.

The measured parameter values (Table 2) demonstrated good consistency between subjects. The reproducibility of the calculated elbow angles from the measured data (Figs. 6–9) for repeated experiments was good. There was also good reproducibility between experiments performed on the same subjects but on different days. An example is shown in blue and green lines for P2 experiment 1 in Fig. 7. The pattern of elbow angle movement from different trials also showed good consistency between subjects.

In the course of the experiment, a number of measurements were taken where the muscle was not fully relaxed and the trajectory of the forearm was clearly different from that when the muscle is fully relaxed. These measurements were not used in the parameter estimation process to obtain results presented in Table 3. The effect of the muscle not being fully relaxed can be seen in the dashed blue line of Fig. 9 (subject P4, Exp 1 0 kg hand load). The initial rate of change is less steep as a result of the active contractile element exerting a resistive force. Importantly, this is clearly distinguishable from the movement of a completely relaxed arm. During the experiments, the subjects were aware of the objective to keep muscle relaxed, and they were asked to report immediately after each measurement if that was not the case. If the subject reported the muscles were not completely relaxed, that measurement was repeated. Whilst in this set of experiments, the effect of muscle tension was obvious, in later studies, EMG was recorded as an objective measure of muscle activation. These data showed that subjects' feedback on whether the muscles were fully relaxed when compared to the EMG or elbow angle time history was found to be reliable. Furthermore, subject feedback is immediately available after each measurement, whilst inspection of the elbow angle time history or EMG can only be carried out after analysis of the data.

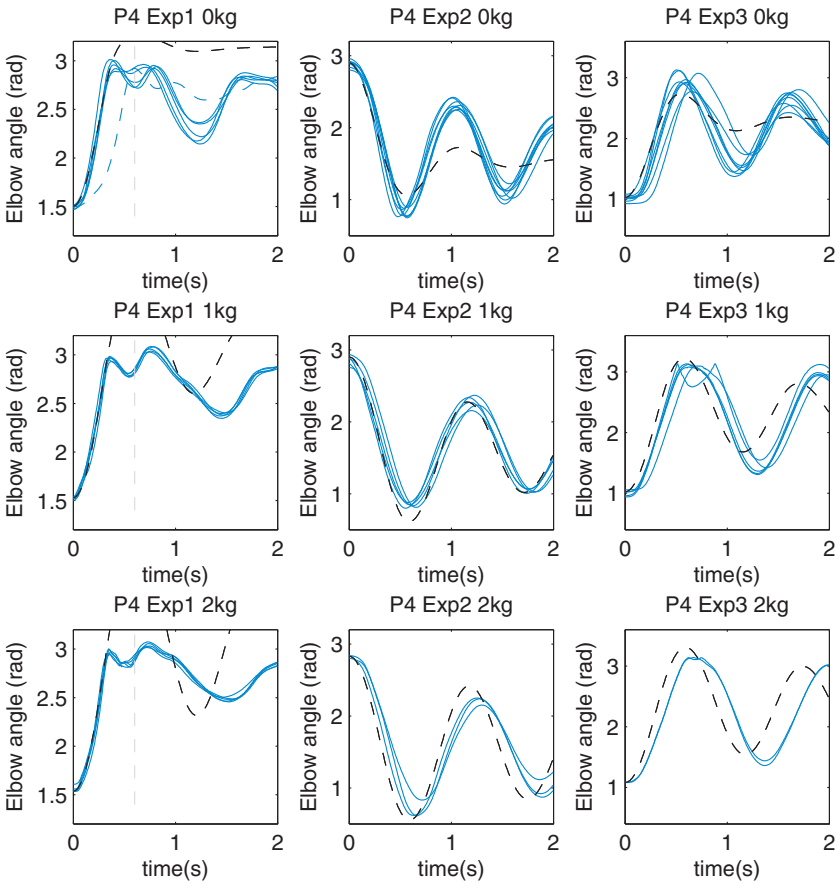

Fig. 9 – Forearm free fall trajectory of subject P4. Blue solids lines: measured joint trajectories. Blue dashed line: measured joint trajectory with muscles not fully relaxed. Black dashed line: simulated joint trajectory using values from Tables 2 and 3. (For interpretation of the references to colour in this figure legend, the reader is referred to the web version of the article.)

7.4. *Parameter estimation*

The root mean square error (RMSE) is a widely used factor to minimise in parameter optimisation. However in the original optimisation process using experiments 1 and 2 [20], it was found that, the standard RMSE calculation did not give equally weighted values if trial lengths were different, and therefore the MAE was used instead. The MAE was used in the optimisation process for the data from experiments 2 and 3 to allow comparison between results from fitting experiments 1 and 2 and fitting experiments 2 and 3.

The duration of data taken for the MAE calculation in both experiments 2 and 3 was 2 s. This was chosen as it included several cycles of oscillation, but was not so long that movement had ceased at the end of the period, as introducing a large number of near zero MAE values during a period of low amplitude movement would reduce the sensitivity of the MAE to differences in the movement dynamics during the initial swings of the arm fall, which was the important factor in the parameter estimation process.

In the preliminary work [26], experiment 1 was used to parameterise the model, where the maximum elbow extension was reached at about 0.4 s and the data up to 0.6 s (grey dashed line, Figs. 6–9) were included so a decrease in elbow angular velocity was present for the parameter estimation and optimisation. However, when experiment 3 was used in the fitting process and compared with the results previously obtained using data from experiment 1, it was found that the difference in elbow angle trajectory characteristics between measured and simulated data at maximum elbow extension in experiment 1 caused the parameter estimation process to result in an unsatisfactory prediction of the elbow angle overall. Therefore in this paper, the MAE was calculated using only measured and simulated data from experiments 2 and 3, and excluded data from experiment 1. This resulted in a better model fit and lower MAE values were obtained.

The use of different seeds in the optimisation process was to help ensure that global minima were found, by ensuring that starting different initial seeds gave the same final values. For subject P4, when the parameter estimation was started with all zero values in the seed, fminsearch reached a local minimum, where the MAE was not as small as those obtained using the other initial seeds. This result was ignored and the global MAE from the other seeds was used. MAE values obtained from the two remaining initial seeds were within 1%, suggesting the fminsearch optimisation process had found global minima. It also suggested that using a physiologically meaningful seed has a higher chance of finding global minima than starting with all zero values.

In this study, fminsearch effectively performed a 7 dimensional grid search to obtain the parameter values. In order to visualise the form of the error surfaces, the MAEs for pairs of variables were plotted. The error surfaces had steep sides with a shallow bowl region around the minimum MAE. These plots confirmed that the estimated parameter values were at the global minimum of the MAE. The shape of these plots also suggested that the model had a low sensitivity to the values.

7.5. *Fitted results*

It can been seen in Figs. 6–9 that the simulated trajectories using the fitted parameter values show good agreement with measured elbow angle trajectories. The values in Table 3 obtained by only using measured data from experiments 2 and 3 for parameter estimation also gave predicted elbow angle trajectories that agree with the initial 0.4 s of measured elbow angle trajectories obtained in experiment 1. This suggests that the fitted values were appropriate for predicting elbow angle for different arm orientations.

The fitted spring and damper values (Table 3) were within the predicted range of values. The fitted values of b_{arm} showed good agreement between all subjects. The muscle spring constants k_{m1} and k_{m2} showed good agreement between subject P1 and P2, however the same values for P3 and P4 showed a large variation. This could be due to uncertainty in the measurement of the muscle and tendon length. In subjects P1 and P2, it was easier to identify the bulk of the muscle by palpation in comparison to P3 and P4, and therefore the error in length determination in P3 and P4 were expected to be greater than in P1 and P2. In Eq. (3) the force generated by muscle spring k_m is dependent on the muscle extension, which is in turn dependent on the measured lengths x_{1_0}, x_{2_0}, x_{1t} and x_{2t}. Therefore any error in those measured lengths will have a corresponding error in the force generated which will affect the parameter optimisation process.

7.6. *Comparison with other work*

It was difficult to compare measured length values between studies because of differences in the definition of the model parameters. For example, the tendon length defined by Winters and Stark [15] includes sheet tendons embedded in the bulk muscle. Hatze's model [23] was similar to the one used in this study, and reported average tricep muscle length of 0.1125 m, which was shorter than all those measured in this study. However the lengths for Hatze's model were obtained through parameter estimation, where the muscle lengths determined were the lengths at which the muscles produced maximum force and not the resting length of the muscles.

No previous studies on the elbow joint reporting passive spring and damping values for the modified Hill muscle model were identified, and therefore, no direct comparison of values could be made. Hof's study [33] on the human tricep surae muscle included a parallel elastic component (PEC) in the muscle model, equivalent to the spring component k_m. However no numerical value for this was reported. Furthermore, based on our previous work [20], Hof's modified Hill model was not uniquely identifiable as both the free tendon (SEC) and the bulk muscle lengths were extendable, and therefore the fitted values could not be guaranteed unique. In our work, the assumption that the free tendon lengths were fixed overcame this problem. In order to develop better models and more robust parameter estimation techniques, more numerical values need to be reported in the literature.

An additional advantage of the passive movement technique in subjects who can produce voluntary movements, is that the parameter values obtained from the passive movement experiment can then be used in studies where the muscle is active (e.g. MVC) to parameterise the force length and force velocity characteristics [16] of the contractile element.

8. Conclusion and future work

Structural identifiability analysis on different versions of Hill type muscle models allowed us to choose a muscle model and determine the constraints (e.g. fixed free tendon length) under which the model parameters can be uniquely identified. When used with measurements from passive movements, the muscles' passive spring and damping elements in the muscle model could be uniquely determined.

In this study, the CE was considered a pure force generator. Since the muscles were completely relaxed in the passive movements, no forces were output from the CE. In MVC studies and other parameter estimation approaches where the muscle is active, the CE force is modulated by the force-length and/or the force–velocity characteristic [16], and therefore parameters for the CE and the spring and damping constants cannot be uniquely determined. Measurements from passive movements allowed the effect of the spring and damping components to be observed and therefore uniquely determined.

Overall, parameter estimation of the musculo-skeletal model from passive movement measurement was successful. By adapting the skeletal model to other joints in the body, such as the knee joint or ankle joint, other muscle groups in the body could be parameterised in a similar manner.

The parameter values obtained from the method described in this paper are for the passive elements of the muscle model, to fully parameterise the model for an active muscle, the force-length and force-velocity characteristics are also required. By combining MVC or other measurement techniques where the muscle is active with the parameter values found using the passive movement method described in this paper, a fully parameterised model of the muscle can be obtained.

Conflict of interest

No benefits in any form have been received or will be received from a commercial party related directly or indirectly to the subject of this article.

Acknowledgments

This work was supported by the Engineering and Physical Sciences Research Council through a Doctoral Training Award. The gait laboratory was obtained through Birmingham Science City Initiative.

REFERENCES

[1] A. Nagano, T. Komura, R. Himeno, S. Fukashiro, A procedure for adjustment of body segmental parameter values to individual subjects in inverse dynamics, International Journal of Sport and Health Science 2 (2004) 156–162.

[2] A.L. Hof, In vivo measurement of the series elasticity release curve of human triceps surae muscle, Journal of Biomechanics 31 (1998) 793–800.

[3] D. Zhang, K. Zhu, Simulation study of FES-assisted standing up with neural network control, Conference Proceedings: Annual International Conference of the IEEE Engineering in Medicine and Biology Society 7 (2004) 4877–4880.

[4] R. Davoodi, B.J. Andrews, Optimal control of FES-assisted standing up in paraplegia using genetic algorithms, Medical Engineering & Physics 21 (1999) 609–617.

[5] P.H. Peckham, J.S. Knutson, Functional electrical stimulation for neuromuscular applications, Annual Review of Biomedical Engineering 7 (2005) 327–360.

[6] M. Bijak, M. Rakos, C. Hofer, W. Mayr, M. Strohhofer, D. Raschka, H. Kern, Stimulation parameter optimization for FES supported standing up and walking in SCI patients, Artificial Organs 29 (2005) 220–223.

[7] G.P. Braz, M. Russold, R.M. Smith, G.M. Davis, Efficacy and stability performance of traditional versus motion sensor-assisted strategies for FES standing, Journal of Biomechanics 42 (2009) 1332–1338.

[8] A.J. Mulder, P.H. Veltink, H.B. Boom, On/off control in FES-induced standing up: a model study and experiments, Medical & Biological Engineering & Computing 30 (1992) 205–212.

[9] R. Riener, T. Fuhr, Patient-driven control of FES-supported standing up: a simulation study, IEEE Transactions on Rehabilitation Engineering 6 (1998) 113–124.

[10] R.P. Jaime, Z. Matjacic, K.J. Hunt, Paraplegic standing supported by FES-controlled ankle stiffness, IEEE Transactions on Neural Systems and Rehabilitation Engineering 10 (2002) 239–248.

[11] A.H. Vette, K. Masani, J.Y. Kim, M.R. Popovic, Closed-Loop Control of Functional Electrical Stimulation-assisted arm-free standing in individuals with spinal cord injury: a feasibility study, Neuromodulation 12 (2009) 22–32.

[12] N.C. Chesler, W.K. Durfee, Surface EMG as a fatigue indicator during FES-induced isometric muscle contractions, Journal of Electromyography and Kinesiology 7 (1997) 27–37.

[13] C. Frigo, M. Ferrarin, W. Frasson, E. Pavan, R. Thorsen, EMG signals detection and processing for on-line control of functional electrical stimulation, Journal of Electromyography and Kinesiology 10 (2000) 351–360.

[14] T. Muramatsu, T. Muraoka, D. Takeshita, Y. Kawakami, Y. Hirano, T. Fukunaga, Mechanical properties of tendon and aponeurosis of human gastrocnemius muscle in vivo, Journal of Applied Physiology 90 (2001) 1671–1678.

[15] J.M. Winters, L. Stark, Estimated mechanical-properties of synergistic muscles involved in movements of a variety of human joints, Journal of Biomechanics 21 (1988) 1027–1041.

[16] A.V. Hill, The heat of shortening and the dynamic constants of muscle, Proceedings of the Royal Society B: Biological Sciences 126 (1938) 136–195.

[17] H.E. Makssoud, D. Guiraud, P. Poignet, 2004 IEEE International Conference on Robotics and Automation, 2004. Proceedings. ICRA '04, 2004.

[18] P.L. Weiss, I.W. Hunter, R.E. Kearney, Human ankle joint stiffness over the full range of muscle activation levels, Journal of Biomechanics 21 (1988) 539–544.

[19] S. Mohammed, P. Poignet, P. Fraisse, D. Guiraud, Toward lower limbs movement restoration with input–output feedback linearization and model predictive control through functional electrical stimulation, Control Engineering Practice 20 (2012) 182–195.

[20] T.F. Yu, A.J. Wilson, Structural identifiability analysis and preliminary parameter estimation for an arm model incorporating the hill muscle model, in: 5th European Conference of the International Federation for Medical and Biological Engineering, vol. 37, 2012, pp. 864–867.

[21] G. Venture, K. Yamane, Y. Nakamura, Identifying musculo-tendon parameters of human body based on the musculo-skeletal dynamics computation and Hill-Stroeve muscle model, in: 2005 5th IEEE-RAS International Conference on Humanoid Robots, 2005, pp. 351–356.

[22] A. Erdemir, S. McLean, W. Herzog, A.J. van den Bogert, Model-based estimation of muscle forces exerted during movements, Clinical Biomechanics 22 (2007) 131–154.

[23] H. Hatze, Estimation of myodynamic parameter values from observations on isometrically contracting muscle groups, European Journal of Applied Physiology and Occupational Physiology 46 (1981) 325–338.

[24] C.Y. Scovil, J.L. Ronsky, Sensitivity of a Hill-based muscle model to perturbations in model parameters, Journal of Biomechanics 39 (2006) 2055–2063.

[25] G. Venture, K. Yamane, Y. Nakamura, In-vivo estimation of the human elbow joint dynamics during passive movements based on the musculo-skeletal kinematics computation, in: 2006 IEEE International Conference on Robotics and Automation (ICRA), vol. 1–10, 2006, pp. 2960–2965.

[26] T.F. Yu, A.J. Wilson, A novel passive movement method for parameter estimation of a musculo-skeletal arm model incorporating a modified hill muscle model, in: Proc. 8th IFAC Symposium on Biological and Medical Systems (IFAC BMS '12), 2012.

[27] C.N. Maganaris, J.P. Paul, In vivo human tendon mechanical properties, Journal of Physiology – London 521 (1999) 307–313.

[28] F.E. Zajac, Muscle and tendon – properties, models, scaling, and application to biomechanics and motor control, Critical Reviews in Biomedical Engineering 17 (1989) 359–411.

[29] Vicon®, Vicon MX System, Vicon Motion Systems, Oxford, UK, 2013 http://www.vicon.com/products/viconmx.html

[30] D.A. Winter, Biomechanics and Motor Control of Human Movement, Wiley, Hoboken, NJ, 2005.

[31] W.M. Murray, T.S. Buchanan, S.L. Delp, The isometric functional capacity of muscles that cross the elbow, Journal of Biomechanics 33 (2000) 943–952.

[32] K.N. An, F.C. Hui, B.F. Morrey, R.L. Linscheid, E.Y. Chao, Muscles across the elbow joint: a biomechanical analysis, Journal of Biomechanics 14 (1981) 659–669.

[33] A.L. Hof, Correcting for limb inertia and compliance in fast ergometers, Journal of Biomechanics 30 (1997) 295–297.